This article is published as part of the *Dalton Transactions* themed issue entitled:

New Talent Asia

Highlighting the excellent work being carried out by younger members of the inorganic academic community in Asia

Guest Editor Masahiro Yamashita
Tohoku University, Japan

Published in issue 10, 2011 of *Dalton Transactions*

Image reproduced with permission of Kenneth Kam-Wing Lo

Articles in the issue include:

PERSPECTIVES:

ARTICLES:

Visit the *Dalton Transactions* website for more cutting-edge inorganic and organometallic research
www.rsc.org/dalton

Celebrating 40 years

Dalton Transactions

An international journal of inorganic chemistry

www.rsc.org/dalton

Volume 40 | Number 10 | 14 March 2011 | Pages 2077–2392

Themed issue: New Talent: Asia

ISSN 1477-9226

RSC Publishing

COVER ARTICLE
Lo *et al.*
Luminescent cyclometallated iridium(III) bis(quinolylbenzaldehyde) diimine complexes

International Year of CHEMISTRY 2011

1477-9226(2011)40:10;1-0

Luminescent cyclometallated iridium(III) bis(quinolylbenzaldehyde) diimine complexes—synthesis, photophysics, electrochemistry, protein cross-linking properties, cytotoxicity and cellular uptake†

Pui-Kei Lee, Hua-Wei Liu, Shek-Man Yiu, Man-Wai Louie and Kenneth Kam-Wing Lo*

Received 19th May 2010, Accepted 28th July 2010
DOI: 10.1039/c0dt00501k

Four new luminescent cyclometallated iridium(III) bis(quinolylbenzaldehyde) diimine complexes $[Ir(qba)_2(N^\wedge N)](PF_6)$ (Hqba = 4-(2-quinolyl)benzaldehyde, N^N = 2,2′-bipyridine, bpy (**1**); 1,10-phenanthroline, phen (**2**); 3,4,7,8-tetramethyl-1,10-phenanthroline, Me_4-phen (**3**); 4,7-diphenyl-1,10-phenanthroline, Ph_2-phen (**4**)) have been synthesised and characterised, and their electronic absorption, emission and electrochemical properties investigated. The X-ray crystal structures of complexes **1** and **2** have been determined. Upon irradiation, complexes **1–4** exhibited intense and long-lived orange-yellow emission in fluid solutions at 298 K and in alcohol glass at 77 K. The emission has been assigned to a triplet intra-ligand (^{3}IL) excited state associated with the qba ligand, probably with mixing of some triplet metal-to-ligand charge-transfer (^{3}MLCT) ($d\pi(Ir) \rightarrow \pi^*(qba)$) character. Reductive amination reactions of complexes **1–4** with the protein bovine serum albumin (BSA) afforded the bioconjugates **1-BSA**–**4-BSA**, respectively. Upon photoexcitation, these bioconjugates displayed intense and long-lived ^{3}MLCT ($d\pi(Ir) \rightarrow \pi^*(N^\wedge C)$) emission in aqueous buffer at 298 K. The cross-linked nature of the Ir–BSA bioconjugates has been verified by SDS-PAGE. Additionally, the cytotoxicity of the complexes towards human cervix epithelioid carcinoma (HeLa) cells has been examined by 3-(4,5-dimethyl-2-thiazolyl)-2,5-diphenyltetrazolium bromide (MTT) assays, and the cellular uptake of complex **4** has been investigated by laser-scanning confocal microscopy and flow cytometry.

Introduction

The rich photophysical and photochemical properties of many transition metal complexes have been well documented. In view of the advantages of these systems such as variable molecular structures, intense absorption and tunable emission in the visible region with high luminescence quantum yields and long emission lifetimes, there is an expanding interest in applying them in biological studies. Recently, the cellular uptake properties and cytotoxicity of polypyridine complexes of platinum(II),[1,2] ruthenium(II),[3–7] rhenium(I),[8–10] rhodium(III)[11] and gold(III)[12] have been widely reported. Since many cyclometallated iridium(III) polypyridine complexes are known to be excellent environment-sensitive emitters,[13–20] this family of complexes are attractive choices for biomolecular and cellular probes.[21,22] Following our interest in the utilisation of cyclometallated iridium(III) polypyridine complexes in biological labelling studies, we anticipate that functionalisation of these luminescent compounds with reactive groups will lead to useful cellular labels and probes.

The main objective of this work is to design new cyclometallated iridium(III) diimine complexes $[Ir(N^\wedge C)_2(N^\wedge N)]^+$ with biological reactivity and desirable photophysical properties for bio-imaging. In this context, compounds that feature both low-energy absorption and emission are attractive candidates as this can minimise the harmful effects of the excitation source and background fluorescence in biological systems, respectively. Additionally, a reactive group such as an aldehyde will render these reagents active towards various amine-containing biological entities. While the first goal can be achieved by introducing an extended planar cyclometallating ligand with lower-lying π* orbitals, the latter target can be accomplished by the incorporation of an aldehyde group into the same ligand. We envisage that new complexes with these characteristics would exhibit desirable absorption and emission in aqueous solutions under ambient conditions owing to significant participation of intraligand (IL) character in the low-lying emissive states,[20c] potential cross-linking properties[20a] as well as unique emission characteristics upon reductive amination *via* the aldehyde groups.[20f] Herein we describe the synthesis, characterisation, photophysics and electrochemistry of four luminescent iridium(III) bis(quinolylbenzaldehyde) diimine complexes $[Ir(qba)_2(N^\wedge N)](PF_6)$ (Hqba = 4-(2-quinolyl)benzaldehyde, N^N = 2,2′-bipyridine, bpy (**1**); 1,10-phenanthroline, phen (**2**); 3,4,7,8-tetramethyl-1,10-phenanthroline, Me_4-phen (**3**); 4,7-diphenyl-1,10-phenanthroline, Ph_2-phen (**4**)) (Chart 1). The bioconjugation products of the protein bovine serum albumin (BSA) modified with these complexes have been studied by emission spectroscopy and SDS-PAGE. Additionally, the cytotoxicity of the complexes towards human cervix epithelioid carcinoma (HeLa) cells has been examined by 3-(4,5-dimethyl-2-thiazolyl)-2,5-diphenyltetrazolium bromide (MTT) assays. Furthermore, the cellular uptake of complex **4** has been investigated by laser-scanning confocal microscopy and flow cytometry.

Department of Biology and Chemistry, City University of Hong Kong, Tat Chee Avenue, Kowloon, Hong Kong, People's Republic of China. E-mail: bhkenlo@cityu.edu.hk; Fax: (+852) 3442 0522; Tel: (+852) 3442 7231

† CCDC reference numbers 775620 and 775621. For crystallographic data in CIF or other electronic format see DOI: 10.1039/c0dt00501k

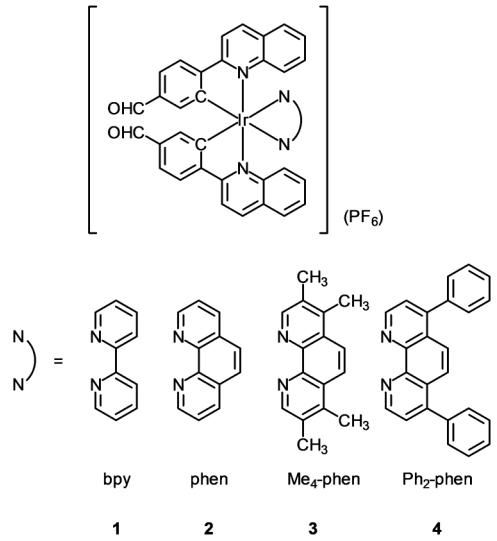

Chart 1 Structures of the iridium(III) complexes.

Experimental

General considerations

All solvents were of analytical reagent grade and purified according to published procedures.[23] All buffer components were of biological grade and used as received. 2-Hydroxyquinoline (Aldrich), *N*-bromosuccinimide (Aldrich), triphenylphosphine (Acros), 4-formylphenylboronic acid (Acros), *cis*-dichlorobis(triphenylphosphine)palladium(II) (Aldrich), K_2CO_3 (Acros), $IrCl_3{\cdot}3H_2O$ (Aldrich), bpy (Aldrich), phen (Acros), Me_4-phen (Acros), Ph_2-phen (Acros) and KPF_6 (Acros) were used without further purification. Hqba was prepared as described previously.[24] BSA was obtained from Calbiochem and used as received. NAP-10 size-exclusion columns and YM-30 microcons were purchased from Pharmacia and Amicon, respectively. HeLa cells were obtained from American Type Culture Collection. Dulbecco's modified Eagle's medium (DMEM), fetal bovine serum (FBS), phosphate buffered saline (PBS), trypsin–EDTA and penicillin/streptomycin were purchased from Invitrogen. The growth medium for cell culture contained DMEM with 10% FBS and 1% penicillin/streptomycin. Sugar-free growth medium (Invitrogen), 2-deoxyglucose (Acros), carbonyl cyanide 3-chlorophenylhydrazone (CCCP) (Acros), potassium nitrate (Acros), sodium azide (Acros), sodium orthovanadate (Acros) and sodium molybdate(VI) dihydrate (Acros) were used without purification.

Synthesis

$[Ir_2(qba)_4Cl_2]$. The synthetic procedure was similar to that reported for related dinuclear iridium(III) complexes.[20a] A mixture of $IrCl_3{\cdot}3H_2O$ (311 mg, 0.88 mmol) and Hqba (548 mg, 2.26 mmol) in 50 ml of 2-ethoxyethanol–water (3 : 1 v/v) was refluxed for 24 h in the dark under an inert atmosphere of nitrogen. The reddish brown precipitate formed was collected by centrifugation and washed with 50 ml of ethanol–water (95 : 5 v/v) and air dried. The solid was then dissolved in CH_2Cl_2 (100 ml) and the solution was filtered with Celite. The filtrate was then evaporated to dryness to give a reddish brown solid. Subsequent recrystallisation from diffusion of diethyl ether into a CH_2Cl_2 solution of $[Ir_2(qba)_4Cl_2]$ afforded reddish brown crystals. The complex was used without further purification. Yield: 379 mg (62%). Positive-ion ESI-MS (*m*/*z*): 656 $\{Ir(qba)_2\}^+$.

$[Ir(qba)_2(N^{\wedge}N)](PF_6)$. A mixture of $[Ir_2(qba)_4Cl_2]$ (83 mg, 0.06 mmol) and N^N (0.26 mmol) in 25 ml of CH_2Cl_2–MeOH–H_2O (2 : 2 : 1 v/v) was heated at reflux under nitrogen for 4 h. The red solution was then cooled to room temperature, and solid KPF_6 (35 mg, 0.19 mmol) was added to the solution. The mixture was then evaporated to dryness, and the solid was dissolved in CH_2Cl_2 and purified by column chromatography on silica gel. The desired product was eluted with CH_2Cl_2–acetone (9 : 1 v/v) and subsequently recrystallised from a mixture of acetone and diethyl ether.

$[Ir(qba)_2(bpy)](PF_6)$ (1). Complex **1** was isolated as red crystals. Yield: 84 mg (80%). ^{1}H NMR (400 MHz, acetone-d_6, 298 K, relative to TMS): δ 9.66 (s, 2H, CHO), 8.72–8.66 (m, 4H, H3 and H4 of quinolyl ring of qba), 8.52 (d, J = 8.1 Hz, 2H, H5 of phenyl ring of qba), 8.47–8.42 (m, 4H, H5, H5′, H6 and H6′ of bpy), 8.17 (dt, J = 8.1 and 1.4 Hz, 2H, H4 of bpy), 8.14 (dd, J = 8.1 and 1.3 Hz, 2H, H5 of quinolyl ring of qba), 7.75–7.72 (m, 4H, H3 and H3′ of bpy and H8 of quinolyl ring of qba), 7.54–7.48 (m, 4H, H6 of phenyl ring and H7 of quinolyl ring of qba), 7.20–7.15 (m, 2H, H6 of quinolyl ring of qba). Anal. Calc. for $C_{42}H_{28}N_4O_2PF_6Ir{\cdot}1/2H_2O$: C, 52.17; H, 3.02; N, 5.79. Found: C, 52.47; H, 3.32; N, 5.54%. IR (KBr) ν/cm^{-1}: 1685 (s, CHO), 839 (s, PF_6^-). Positive-ion ESI-MS (*m*/*z*): 813 $\{M - PF_6^-\}^+$.

$[Ir(qba)_2(phen)](PF_6)$ (2). Complex **2** was isolated as orange-red crystals. Yield: 148 mg (72%). ^{1}H NMR (400 MHz, acetone-d_6, 298 K, relative to TMS): δ 9.70 (s, 2H, CHO), 8.82 (dd, J = 5.1 and 1.4 Hz, 2H, H2 and H9 of phen), 8.78 (dd, J = 8.3 and 1.4 Hz, 2H, H4 and H7 of phen), 8.73 (d, J = 8.9 Hz, 2H, H4 of quinolyl ring of qba), 8.62 (d, J = 8.9 Hz, 2H, H3 of quinolyl ring of qba), 8.58 (d, J = 8.2 Hz, 2H, H5 of phenyl ring of qba), 8.13 (s, 2H, H5 and H6 of phen), 8.10 (dd, J = 8.3 and 5.1 Hz, 2H, H3 and H8 of phen), 7.88 (dd, J = 8.2 and 1.4 Hz, 2H, H5 of quinolyl ring of qba), 7.79 (dd, J = 8.1 and 1.6 Hz, 2H, H8 of quinolyl ring of qba), 7.41 (d, J = 9.0 Hz, 2H, H6 of phenyl ring of qba), 7.37–7.33 (m, 2H, H7 of quinolyl ring of qba), 7.30 (d, J = 1.4 Hz, 2H, H2 of phenyl ring of qba), 6.95–6.91 (m, 2H, H6 of quinolyl ring of qba). Anal. Calc. for $C_{44}H_{28}N_4O_2PF_6Ir$: C, 53.82; H, 2.88; N, 5.71. Found: C, 53.66; H, 2.94; N, 5.76%. IR (KBr) ν/cm^{-1}: 1683 (s, CHO), 845 (s, PF_6^-). Positive-ion ESI-MS (*m*/*z*): 837 $\{M - PF_6^-\}^+$.

$[Ir(qba)_2(Me_4\text{-phen})](PF_6)$ (3). Complex **3** was isolated as orange-red crystals. Yield: 60.3 mg (65%). ^{1}H NMR (400 MHz, acetone-d_6, 298 K, relative to TMS): δ 9.68 (s, 2H, CHO), 8.74 (d, J = 8.8 Hz, 2H, H4 of quinolyl ring of qba), 8.61 (d, J = 8.6 Hz, 2H, H3 of quinolyl ring of qba), 8.58 (d, J = 8.2 Hz, 2H, H5 of phenyl ring of qba), 8.45 (s, 2H, H2 and H9 of Me_4-phen), 8.23 (s, 2H, H5 and H6 of Me_4-phen), 7.88 (dd, J = 8.1 and 5.4 Hz, 2H, H5 of quinolyl ring of qba), 7.77 (dd, J = 8.1 and 1.6 Hz, 2H, H8 of quinolyl ring of qba), 7.44 (d, J = 8.9 Hz, 2H, H6 of phenyl ring of qba), 7.36–7.32 (m, 2H, H7 of quinolyl ring of qba), 7.23 (d, J = 1.5 Hz, 2H, H2 of phenyl ring of qba), 6.93–6.91 (m, 2H, H6 of quinolyl ring of qba), 2.78 (s, 6H, CH_3 on C4 and C7 of Me_4-phen), 2.45 (s, 6H, CH_3 on C3 and C8 of Me_4-phen).

Anal. Calc. for $C_{48}H_{36}N_4O_2PF_6Ir{\cdot}H_2O$: C, 54.59; H, 3.63; N, 5.31. Found: C, 54.73; H, 3.87; N, 5.44%. IR (KBr) ν/cm^{-1}: 1668 (s, CHO), 845 (s, PF_6^-). Positive-ion ESI-MS ion cluster (m/z): 893 $\{M - PF_6^-\}^+$.

[Ir(qba)$_2$(Ph$_2$-phen)](PF$_6$) (4). Complex **4** was isolated as orange crystals. Yield: 54 mg (42%). ^{1}H NMR (400 MHz, acetone-d_6, 298 K, relative to TMS): δ 9.71 (s, 2H, CHO), 8.89 (d, J = 5.4 Hz, 2H, H2 and H9 of Ph$_2$-phen), 8.76 (d, J = 4.4 Hz, 2H, H4 of quinolyl ring of qba), 8.66 (d, J = 8.7 Hz, 2H, H3 of quinolyl ring of qba), 8.60 (d, J = 8.2 Hz, 2H, H5 of phenyl ring of qba), 8.07 (d, J = 5.4 Hz, 2H, H3 and H8 of Ph$_2$-phen), 8.03 (s, 2H, H5 and H6 of Ph$_2$-phen), 7.93 (d, J = 8.3 Hz, 2H, H5 of quinolyl ring of qba), 7.80 (d, J = 8.3 Hz, 2H, H8 of quinolyl ring of qba), 7.63–7.51 (m, C_6H_5 on C4 and C7 of Ph$_2$-phen and H6 of phenyl ring of qba), 7.42–7.38 (m, 2H, H7 of quinolyl ring of qba), 7.30 (d, J = 1.4 Hz, 2H, H2 of phenyl ring of qba), 7.09–7.05 (m, 2H, H6 of quinolyl ring of qba). Anal. Calc. for $C_{54}H_{48}N_4O_2PF_6Ir$: C, 57.80; H, 4.31; N, 4.99. Found: C, 57.76; H, 4.52; N, 5.10%. IR (KBr) ν/cm^{-1}: 1687 (s, CHO), 845 (s, PF_6^-). Positive-ion ESI-MS (m/z): 977 $\{M - PF_6^-\}^+$.

Physical measurements and instrumentation

Instruments for the characterisation and photophysical and electrochemical measurements have been described previously.[22] Luminescence quantum yields were measured using the optically dilute method[25] with an aerated aqueous solution of $[Ru(bpy)_3]Cl_2$ (Φ_{em} = 0.028) as the standard solution.[26]

Crystal structure determination

X-Ray structural analysis of complex 1. Single crystals of complex **1** suitable for X-ray crystallographic studies were obtained by slow diffusion of diethyl ether vapour into a concentrated acetone solution of the complex. A crystal of dimensions 0.58 × 0.15 × 0.12 mm coated with paratone-N and mounted on a nylon cryoloop was used for X-ray diffraction analysis. X-ray diffraction data were collected on an Oxford Diffraction Gemini S Ultra 4-circle kappa diffractometer with a 92 mm diagonal Sapphire CCD detector using graphite monochromatised Mo-Kα radiation at 133 K. Data collection was made with a 1° oscillation step of ω, a 20 s exposure time and a detector distance of 60 mm. A total of 1117 frames in 17 runs were collected. The images were interpreted and intensities integrated using the programme CrysAlis.[27] The structure was solved and refined using full-matrix least-squares based on F^2 with the programmes SHELXS-97[28] and SHELXL-97[28] within WinGX[29] on a PC. Iridium and many non-hydrogen atoms were located according to direct methods. The positions of other non-hydrogen atoms were found after successful refinement by full-matrix least-squares using SHELXL-97. One crystallographic asymmetric unit consists of one Ir formula unit, one PF_6 anion and half a diethyl ether solvent molecule. In the final stage of least-squares refinement, non-hydrogen atoms on the disordered diethyl ether solvent molecule and the disordered formyl group on one of the qba ligands were refined isotropically and the other non-hydrogen atoms were refined anisotropically. Hydrogen atoms were generated by SHELXL-97. The positions of the hydrogen atoms were calculated on the basis of riding mode with thermal parameters equal to 1.2 times that of the associated C atoms, and participated in the calculation of final R-indices. Crystal data and a summary of data collection and refinement details are given in Table 1.

Table 1 Crystal data and summary of data collection and refinement for complexes **1** and **2**

	1	**2**
Empirical formula	$C_{42}H_{28}F_6IrN_4O_2P{\cdot}C_2H_5O_{0.50}$	$C_{44}H_{28}F_6IrN_4O_2P{\cdot}C_{6.50}H_{14}O_2$
M_r	994.91	1106.05
Crystal size/mm	0.58 × 0.15 × 0.12	0.64 × 0.28 × 0.16
T/K	133	173
Crystal system	Triclinic	Triclinic
Space group	$P\bar{1}$	$P\bar{1}$
a/Å	10.6285(3)	11.1167(3)
b/Å	13.1359(3)	12.1327(4)
c/Å	14.5805(3)	16.8271(5)
V/Å^3	1895.12(7)	2202.76(12)
Z	2	2
ρ_c/g cm^{-3}	1.744	1.668
μ/mm^{-1}	3.64	3.15
F/000	982	1102
θ range/°	3.6–32.2	3.4–27.5
Oscillation/°	1	1
Distance/mm	60	55
Exposure time/s	20	10
Index ranges	$-12 \le h \le 12$; $-15 \le k \le 15$; $-17 \le l \le 17$	$-13 \le h \le 11$; $-14 \le k \le 14$; $-19 \le l \le 20$
R_{int}[a]	0.025	0.019
No. of unique data/restraints/parameters	6659/4/523	7729/70/646
GOF on F^2[b]	1.07	0.98
R_1, wR_2 ($I > 2\sigma(I)$)[c]	0.0170, 0.0447	0.0209, 0.0469
R_1, wR_2 (all data)	0.0193, 0.0452	0.0258, 0.0476
Largest diff. peak, hole/e Å^{-3}	1.12, –0.46	1.11, –0.69

[a] $R_{int} = \Sigma\,|F_o^2 - F_o^2\,(\text{mean})|\,/\Sigma[F_o^2]$. [b] GOF = $\{\Sigma[w(F_o^2 - F_c^2)^2]/(n - p)\}^{1/2}$, where n is the number of reflections and p is the total number of parameters refined. The weighting scheme is $w = 1/[\sigma^2(F_o^2) + (0.0321P)^2 + 0.1169P]$ for complex **1** and $w = 1/[\sigma^2(F_o^2) + (0.0028P)^2]$ for complex **2**, where P is $(F_o^2 + 2F_c^2)]/3$. [c] $R_1 = \Sigma\,||F_o| - |F_c||/\Sigma\,|F_o|$, $wR_2 = \{\Sigma[w(F_o^2 - F_c^2)^2]/\Sigma[w(F_o^2)]\}^{1/2}$.

X-Ray structural analysis of complex 2. Single crystals of complex **2** suitable for X-ray crystallographic studies were obtained by slow diffusion of diethyl ether vapour into a concentrated acetone solution of the complex. A crystal of dimensions 0.64 × 0.28 × 0.16 mm coated with paratone-N and mounted on a nylon cryoloop was used for X-ray diffraction analysis. X-ray diffraction data were collected on an Oxford Diffraction Gemini S Ultra 4-circle kappa diffractometer with a 92 mm diagonal Sapphire CCD detector using graphite monochromatised Mo-Kα radiation at 173 K. Data collection was made with a 1° oscillation step of ω, a 10 s exposure time and a detector distance at 55 mm. A total of 422 frames in 5 runs were collected. The images were interpreted and intensities integrated using the programme CrysAlis. The structure was solved and refined using full-matrix least-squares based on F^2 with the programmes SHELXS-97 and SHELXL-97 within WinGX. Iridium and many non-hydrogen atoms were located according to direct methods. The positions of other non-hydrogen atoms were found after successful refinement by full-matrix least-squares using SHELXL-97 on a PC. One

crystallographic asymmetric unit consists of one Ir formula unit, one PF_6 anion, one acetone solvent molecule and half an acetone and half a diethyl ether solvent molecule occupying the same void. In the final stage of least-squares refinement, all non-hydrogen atoms were refined anisotropically. Hydrogen atoms were generated by the programme SHELXL-97. The positions of the hydrogen atoms were calculated on the basis of riding mode with thermal parameters equal to 1.2 or 1.5 times that of the associated C atoms, and participated in the calculation of final *R*-indices. Crystal data and a summary of data collection and refinement details are given in Table 1.

Conjugation of BSA with complexes 1–4

In a typical procedure, the iridium(III) complex (1 mg) in anhydrous DMSO (20 μl) was added to BSA (5 mg) dissolved in 50 mM carbonate buffer at pH 10.0 (180 μl). After the mixture was gently stirred in the dark for 6 h, $NaCNBH_3$ (0.63 mg, 10 μmol) in 2 μl of 2 M NaOH was added, and the mixture was stirred gently in the dark for 12 h at room temperature. Then, the mixture was diluted with 50 mM phosphate buffer at pH 7.4 and the precipitate was removed by centrifugation. The filtrate was loaded to a PD-10 size-exclusion column that had been equilibrated with 50 mM phosphate buffer at pH 7.4. The same buffer was used as the mobile phase, and the first band with strong orange-yellow emission was collected, concentrated with a YM-30 microcon and stored at 4 °C before use.

SDS-PAGE

The Ir-BSA bioconjugate ([BSA] = *ca.* 10 mg ml^{-1}; 10 μl) was mixed with a sample buffer (25% glycerol, 5% β-mercaptoethanol, 2% SDS and 0.01% bromophenol blue in 0.06 M Tris-HCl at pH 6.8; 10 μl). The mixture was denatured at 95 °C for 5 min before being loaded into a 6% polyacrylamide gel for SDS-PAGE analysis (Bio-Rad electrophoresis accessories). The gel was directly imaged using a Fujifilm LAS-4000 luminescent image analyser with excitation at 460 nm.

Cytotoxicity assays

HeLa cells were seeded in a 96-well flat-bottomed microplate (10,000 cells $well^{-1}$) in growth medium (100 μl) and incubated at 37 °C under a 5% CO_2 atmosphere for 24 h. The iridium(III) complexes and cisplatin (positive control) were then added, respectively, to the wells with concentrations ranging from *ca.* 10^{-7} to 10^{-4} M in a mixture of growth medium–DMSO (99 : 1 v/v). Wells containing growth medium without cells were used as blank controls. The microplate was incubated at 37 °C under a 5% CO_2 atmosphere for 48 h. Then, 10 μL of MTT in PBS (5 mg ml^{-1}) was added to each well. The microplate was incubated at 37 °C under a 5% CO_2 atmosphere for another 3 h. The medium in each well was then removed, and 100 μl of isopropanol was added to each well and the microplate was further incubated for 5 min. The absorbance of the solutions at 570 nm was measured with a SPECTRAmax 340 microplate reader (Molecular Devices Corp., Sunnyvale, CA, USA). The IC_{50} values of the complexes were determined from dose dependence of surviving cells after exposure to the complexes.

Flow cytometry

HeLa cells in growth medium (100,000 cells ml^{-1}) were seeded in a 35 mm tissue culture dish and incubated at 37 °C under a 5% CO_2 atmosphere for 48 h. The culture medium was removed and replaced with medium–DMSO (99 : 1 v/v) containing the iridium(III) complexes at a concentration of 5 μM. After incubation for 1 h, the medium was removed, and the cell layer was washed gently with PBS (1 ml × 3). The cell layer was then trypsinised and made up to a final volume of 1 ml with PBS. The samples were analysed by a FACSCalibur flow cytometer (Becton, Dickinson and Co., Franklin Lakes, NJ, USA) with excitation at 488 nm. The number of cells analysed for each sample was between *ca.* 9,000 and 10,000.

Live-cell confocal imaging

HeLa cells were grown on sterile glass coverslips in a 35 mm tissue culture dish. The sample preparation procedure was similar to that of the flow cytometry. After washing with PBS, the coverslips were mounted onto slides for measurements. Imaging was performed using a confocal microscope (Carl Zeiss, LSM510) with an excitation wavelength at 488 nm. The emission intensity was measured between 505 and 800 nm.

Fixed-cell confocal imaging

The incubation procedure was similar to that of live-cell confocal imaging except that after washing with PBS, the coverslips were incubated in (1) MeOH–PBS (1 : 1 v/v) for 4 min and then in MeOH for 4 min, or (2) 10% paraformaldehyde for 10 min and then washed successively with MeOH. The coverslips were finally washed with PBS before being mounted onto the slides for measurements.

ICP-MS

HeLa cells were grown in a 60 mm tissue culture dish and incubated at 37 °C under a 5% CO_2 atmosphere for 48 h. The culture medium was then removed and replaced with medium–DMSO (99 : 1 v/v) containing the iridium(III) complexes at a concentration of 5 μM. After incubating for 1 h, the medium was removed, and the cell layer was washed gently with PBS (1 ml × 3). The cell layer was then trypsinised and made up to a final volume of 1 ml with PBS. The harvested cells were digested with 65% HNO_3 (2 ml) at 60 °C for 1 h, and then diluted in Milli-Q water to a final volume of 10 ml. The concentration of iridium was measured using an Elan 6100 DRC-ICP-MS system (PerkinElmer SCIEX Instruments, USA) equipped with a peristaltic pump, Meinhard quartz nebuliser, cyclonic spray chamber, nickel skimmer, and sample cones.

Results and discussion

Synthesis

The dimeric precursor compound $[Ir_2(qba)_4Cl_2]$ was synthesised, in a moderate yield, from the reaction of $IrCl_3 \cdot 3H_2O$ and excess Hqba ligand. The complex was isolated as reddish brown crystals after recrystallisation from a mixture of CH_2Cl_2 and diethyl ether. The mononuclear iridium(III) complexes **1–4** were obtained from

the reactions of the dinuclear complex with two equivalents of the corresponding diimine ligands. These four complexes were isolated as air-stable orange-red crystals in good yields. They were characterised by ^{1}H NMR spectroscopy, positive-ion ESI-MS and IR spectroscopy, and gave satisfactory microanalysis. The aldehyde moieties of complexes **1–4** were characterised by a singlet at *ca.* $\delta = 9.7$ ppm in the ^{1}H NMR spectra and an intense IR absorption band at *ca.* 1685 cm^{-1}. The crystal structures of complexes **1** and **2** have also been studied by X-ray crystallography.

X-Ray crystal structure determination

The perspective views of the cations of complexes **1** and **2** are depicted in Fig. 1 and 2, respectively. Selected bond lengths and angles are listed in Table 2. In both complexes, the iridium(III) centre adopted a distorted octahedral geometry, and the angles of the *trans* ligands at the metal centre ranged from 168.59(8) to 170.19(8) Å for complex **1** and from 168.17(9) to 169.71(10) Å for complex **2**. The coordination geometry of the qba ligands around the iridium(III) centre was such that the metal–carbon bonds were in a *cis* orientation.[16,20a,b,22d] The *trans* influence of the carbon donors rendered slightly longer Ir–N bond lengths in the N^N ligands (Ir1–N3 and Ir1–N4; 2.173(2) and 2.1657(19) Å for complex **1** and Ir1–N3 and Ir–N4; 2.197(2) and 2.172(2) Å for complex **2**) than those in the qba ligands (Ir1–N1 and Ir1–N2; 2.096(2) and 2.091(2) Å for complex **1** and Ir1–N1 and Ir1–N2; 2.091(2) Å for complex **2**). The bite angles of the qba ligands (79.17(9) and 79.61(9)° for complex **1** and 79.67(10) and 79.56(10)° for complex **2**) were larger than those of the N^N ligands (74.99(8)° for complex **1** and 75.88(9)° for complex **2**). These observations have been made in related cyclometallated iridium(III) polypyridine systems $[Ir(N^C)_2(N^N)]^+$.[16,20a,b,22d] The distance between the oxygen atoms of the two aldehyde groups was *ca.* 9.7 Å for complex **1** and 9.6 Å for complex **2**, respectively.

Table 2 Selected bond lengths (Å) and angles (°) for complexes **1** and **2**

Complex **1**			
Ir1–C21	1.993(2)	Ir1–N1	2.096(2)
Ir1–C6	1.998(2)	Ir1–N4	2.1657(19)
Ir1–N2	2.091(2)	Ir1–N3	2.173(2)
C21–Ir1–C6	92.27(9)	N2–Ir1–N4	83.52(7)
C21–Ir1–N2	79.61(9)	N1–Ir1–N4	105.72(8)
C6–Ir1–N2	92.44(9)	C21–Ir1–N3	168.59(8)
C21–Ir1–N1	94.42(9)	C6–Ir1–N3	97.63(9)
C6–Ir1–N1	79.17(9)	N2–Ir1–N3	105.50(8)
N2–Ir1–N1	169.57(7)	N1–Ir1–N3	81.96(8)
C21–Ir1–N4	95.77(8)	N4–Ir1–N3	74.99(8)
C6–Ir1–N4	170.19(8)		
Complex **2**			
Ir1–C17	1.987(3)	Ir1–N2	2.091(2)
Ir1–C1	1.996(3)	Ir1–N4	2.172(2)
Ir1–N1	2.091(2)	Ir1–N3	2.197(2)
C17–Ir1–C1	93.50(11)	N1–Ir1–N4	104.22(9)
C17–Ir1–N1	93.62(10)	N2–Ir1–N4	84.85(8)
C1–Ir1–N1	79.67(10)	C17–Ir1–N3	168.17(9)
C17–Ir1–N2	79.56(10)	C1–Ir1–N3	95.61(10)
C1–Ir1–N2	92.38(10)	N1–Ir1–N3	80.64(8)
N1–Ir1–N2	169.26(8)	N2–Ir1–N3	107.53(9)
C17–Ir1–N4	95.73(10)	N4–Ir1–N3	75.88(9)
C1–Ir1–N4	169.71(10)		

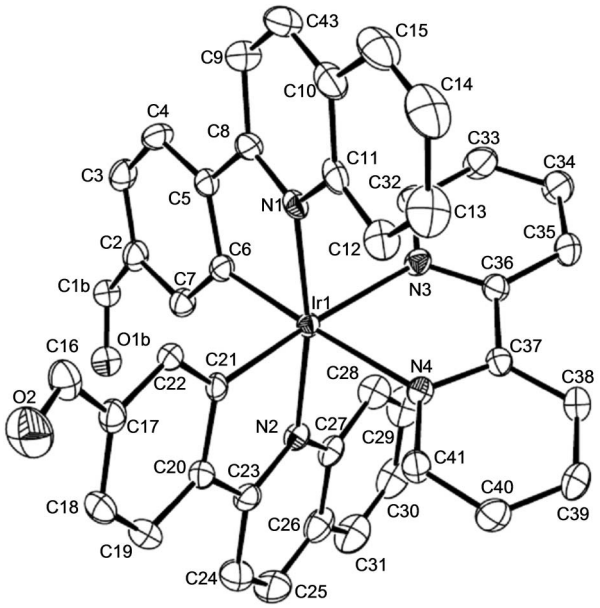

Fig. 1 Perspective view of the cation of complex **1**. Thermal ellipsoids are set at the 50% probability level. Hydrogen atoms are omitted for clarity.

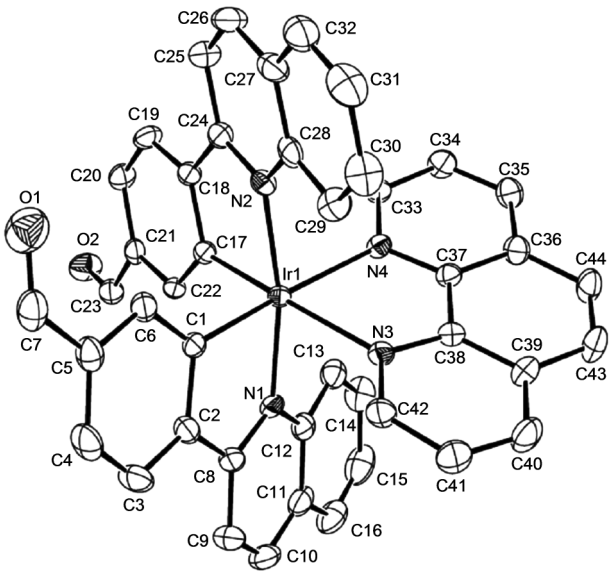

Fig. 2 Perspective view of the cation of complex **2**. Thermal ellipsoids are set at the 50% probability level. Hydrogen atoms are omitted for clarity.

Electronic absorption and luminescence properties

The electronic absorption spectral data of complexes **1–4** in CH_2Cl_2 and CH_3CN at 298 K are listed in Table 3. The electronic absorption spectra of complexes **1** and **4** in CH_3CN at 298 K are displayed in Fig. 3. Complexes **1–3** showed intense absorption features in the UV region (ε on the order of 10^4 dm^3 mol^{-1} cm^{-1}) and moderate absorption bands in the visible region. With reference to the photophysical studies of related cyclometallated iridium(III) polypyridine systems,[14–17,19,20a–e,22] the high-energy absorption bands at *ca.* 256–320 nm have been assigned to spin-allowed ^{1}IL transitions ($\pi \rightarrow \pi^*$) (qba and diimine), whereas the low-energy absorption shoulders at *ca.* 388–478 nm have been assigned to spin-allowed metal-to-ligand charge-transfer

Table 3 Electronic absorption spectral data of the iridium(III) complexes at 298 K

Complex	Medium	λ_{abs}/nm (ε/dm^3 mol^{-1} cm^{-1})
1	CH_2Cl_2	250 (38805), 273 sh (51760), 284 (60040), 293 sh (56225), 308 sh (32225), 342 (31290), 358 sh (27185), 451 (5660), 488 sh (3080), 551 (300)
	CH_3CN	246 sh (38120), 282 (59310), 292 sh (54270), 339 (29900), 354 sh (26515), 391 sh (5935), 450 (5225), 484 sh (2880), 550 (280)
2	CH_2Cl_2	252 sh (40510), 279 (73850), 292 sh (62255), 322 sh (26780), 341 (32015), 356 (31125), 451 (6485), 487 sh (3220), 551 (325)
	CH_3CN	231 sh (46430), 278 (65195), 292 sh (51625), 341 (28135), 355 sh (26740), 389 sh (6870), 448 (5460), 483 sh (2815), 550 (310)
3	CH_2Cl_2	271 sh (56545), 282 (71625), 295 sh (53430), 342 (29065), 357 sh (26325), 388 sh (7505), 414 sh (4805), 454 (4870), 486 sh (2865), 551 (330)
	CH_3CN	235 sh (49095), 282 (78485), 339 (31055), 355 sh (27485), 391 sh (7270), 453 (5040), 488 sh (2670), 553 (315)
4	CH_2Cl_2	272 sh (53845), 285 (72085), 293 sh (67795), 341 sh (31945), 356 (28290), 386 sh (11890), 451 (5580), 487 sh (2810), 551 (290)
	CH_3CN	225 sh (59180), 284 (83390), 341 sh (34570), 355 sh (31200), 389 sh (10550), 448 (5990), 486 sh (2770), 550 (305)

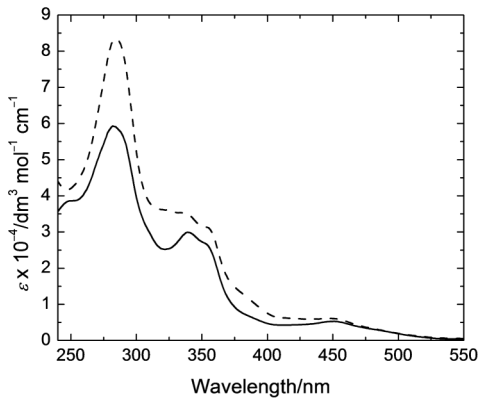

Fig. 3 Electronic absorption spectra of complexes **1** (—) and **4** (---) in CH_3CN at 298 K.

(^{1}MLCT) transitions (dπ(Ir) → π*(qba and diimine)). Although similar assignments have been made for complex **4**, the absorption shoulders of complex **4** have substantial ^{1}IL character due to the lower-lying π* orbitals of Ph_2-phen.[14–17,19,20a–e,22] The spectra of all four complexes exhibited weaker absorption tails towards the lower energy region, which may be attributed to spin-forbidden ^{3}MLCT (dπ(Ir) → π*(qba and diimine)) transitions.[14–17,19,20a–e,22]

Photoexcitation of complexes **1–4** resulted in strong and long-lived orange-yellow luminescence in fluid solutions under ambient conditions and in low-temperature alcohol glass. The photophysical data are summarised in Table 4. The emission spectra of complex **4** are shown in Fig. 4. In fluid solutions at room temperature, all four complexes displayed structured and indistinguishable emission spectra with an emission maximum at *ca.* 573–581 nm and a shoulder at *ca.* 621–624 nm. The emission lifetimes of complexes **1–4** were single-exponential (*ca.* 2.4 to 2.7 μs) and about one order of magnitude longer than those of common cyclometallated iridium(III) polypyridine systems. The

Table 4 Photophysical data of the iridium(III) complexes

Complex	Medium (T/K)	λ_{em}/nm	τ_o/μs	Φ
1	CH_2Cl_2 (298)	573, 621 sh	2.67	0.36
	CH_3CN (298)	577, 622 sh	2.56	0.34
	Glass[a] (77)	565 (max), 615, 670 sh	4.40	
2	CH_2Cl_2 (298)	575, 621 sh	2.58	0.43
	CH_3CN (298)	577, 623 sh	2.49	0.29
	Glass[a] (77)	566 (max), 614, 669 sh	4.41	
3	CH_2Cl_2 (298)	577, 621 sh	2.43	0.38
	CH_3CN (298)	581, 623 sh	2.50	0.29
	Glass[a] (77)	568 (max), 617, 671 sh	4.65	
4	CH_2Cl_2 (298)	575, 621 sh	2.52	0.38
	CH_3CN (298)	577, 624 sh	2.49	0.27
	Glass[a] (77)	566 (max), 613, 672 sh	4.45	

[a] EtOH–MeOH (4 : 1 v/v).

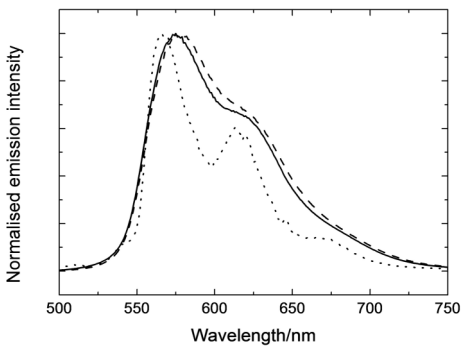

Fig. 4 Emission spectra of complex **4** in CH_2Cl_2 (—) and in CH_3CN (---) at 298 K and in EtOH–MeOH (4 : 1 v/v) at 77 K (···).

independence of the emission energy on the identity of the diimine ligands, together with the observation of structured emission features, long emission lifetimes and high luminescence quantum yields, suggest that the emission of complexes **1–4** in fluid solutions is derived from an ^{3}IL (π → π*) (qba) excited state, perhaps with mixing of some ^{3}MLCT (dπ(Ir) → π*(qba)) character.[14,16–18,19b,20,22] This is supported by the red-shifted emission energy of complexes **1–4** compared to their pba (Hpba = 4-(2-pyridyl)benzaldehyde) counterparts [Ir(pba)$_2$(N^N)](PF$_6$) (N^N = bpy, phen, Me$_4$-phen, Ph$_2$-phen)[20a] owing to the more π-conjugated cyclometallating ligand qba. In alcohol glass at 77 K, the structural features in the emission spectra of complexes **1–4** became more evident. Again, the emission decays followed first-order kinetics, with a lifetime of *ca.* 4.4–4.7 μs. The blue shifts of complexes **1–4** were relatively small, and the emission energy was independent of the nature of the diimine ligands. Thus, it is likely that the low-temperature glass emission of complexes **1–4**, similar to their emission in solutions, originated from an excited state of predominant ^{3}IL (π → π*) (qba) character,[14,16–18,19b,20,22] although the existence of some ^{3}MLCT (dπ(Ir) → π*(qba)) character cannot be ruled out.

Electrochemical properties

The electrochemical properties of the cyclometallated iridium(III) polypyridine complexes have been studied by cyclic voltammetry. The electrochemical data are listed in Table 5. The cyclic voltammograms of complex **1** are displayed in Fig. 5. All the complexes showed a reversible couple at *ca.* +1.41 to +1.46 V *vs.* SCE, which has been assigned to the iridium(IV/III)

Table 5 Electrochemical data of the iridium(III) complexes[a]

Complex	Oxidation $E_{1/2}$/V	Reduction $E_{1/2}$ or E_c/V
1	+1.46	−1.25, −1.43, −1.68, −1.85,[b] −2.06[b]
2	+1.46	−1.24, −1.42, −1.66, −1.87,[b] −2.06[b]
3	+1.41	−1.27, −1.47, −1.75 −1.90,[b], −2.07[b]
4	+1.45	−1.24, −1.41, −1.59, −1.80[b], −2.02[b]

[a] In CH_3CN (0.1 M TBAP) at 298 K (glassy carbon working electrode, sweep rate = 100 mV s^{-1}, all potentials *vs.* SCE). [b] Irreversible waves.

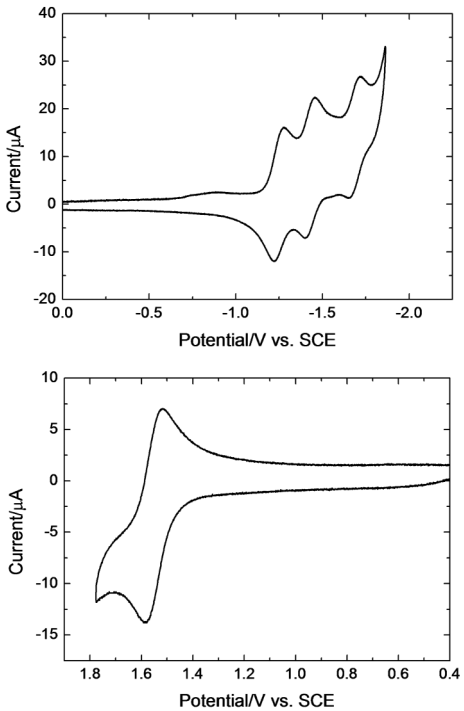

Fig. 5 Cyclic voltammograms of complex **1** in CH_3CN at 298 K.

oxidation couple.[13–19,20a–e,22a–f] With reference to previous electrochemical studies of related cyclometallated iridium(III) polypyridine complexes,[14,16,18,19b,20a–e,22a–f] the first reversible reduction couple of all the complexes at *ca.* −1.24 to −1.27 V has been assigned to the reduction of one of the qba ligands, which is in agreement with the photophysical data that the LUMOs of the complexes should be the qba ligands. Additionally, all the complexes displayed more reduction waves at more negative potentials, which have been assigned to the reduction of the diimine and cyclometallating ligands.[14,16,18,19b,20a–e,22a–f]

Conjugation of BSA

Since the aldehyde group can react readily with a primary amine group to form a secondary amine after reductive amination, complexes **1–4** are considered as amine-specific biological labelling reagents. We have conjugated the protein BSA with complexes **1–4**. The electronic absorption spectra of the bioconjugates **1-BSA–4-BSA** revealed intense absorption at 280 nm, attributable to both the protein and complex absorption, and other absorption features in the visible region mainly due to the iridium(III) complexes. The dye-to-protein ratios (*D*/*P*) determined from the electronic absorption spectra of the free complexes and bioconjugates are

Table 6 Photophysical data of the bioconjugates in 50 mM potassium phosphate buffer pH 7.4 at 298 K

Conjugates	λ_{em}/nm	τ_o/μs	Φ
1-BSA	586	0.42 (16%), 1.28 (84%)	0.10
2-BSA	587	0.44 (16%), 1.25 (84%)	0.086
3-BSA	593	0.29 (15%), 1.06 (85%)	0.039
4-BSA	589	0.41 (16%), 1.23 (84%)	0.098

ca. 0.3–0.9. Upon photoexcitation, the bioconjugates **1-BSA–4-BSA** exhibited moderately intense long-lived yellow emission in 50 mM potassium phosphate buffer pH 7.4 at 298 K (Table 6). The emission spectra of these labelled proteins in aqueous buffer displayed structureless bands *ca.* 586–593 nm, which were at lower energies compared to those of the free complexes in organic solvents. The emission has been tentatively assigned to a ^{3}MLCT ($d\pi(Ir) \rightarrow \pi^*(N^\wedge C)$) excited state mixed with a ^{3}IL ($\pi \rightarrow \pi^*$) ($N^\wedge C$) character. The emission lifetimes of the bioconjugates were biexponential (*ca.* 0.29–1.28 μs), which were not uncommon for proteins labelled with transition metal complexes. Additionally, the luminescent bioconjugates have been analyzed by SDS-PAGE. The results of the analysis are shown in Fig. 6. Upon photoexcitation, all the Ir–BSA bioconjugates displayed several luminescent bands on the gel. The brightest bands corresponded to a molecular weight close to that of BSA (MW = 66 kDa), indicating that the molecular weight of the labelled protein was not altered much by the iridium(III) complex. Additionally, the other bands have been ascribed to the labelled dimer (MW = *ca.* 132 kDa) as well as other oligomers (Fig. 6). The two amine-reactive aldehyde moieties of each molecule of the iridium(III) complexes rendered them useful luminescent cross-linkers for biomolecules such as the model protein BSA in this study.

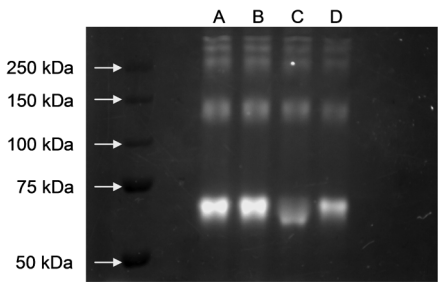

Fig. 6 Results of SDS-PAGE of the Ir–BSA bioconjugates. Lanes A–D are **1-BSA**, **2-BSA**, **3-BSA** and **4-BSA**, respectively.

Cytotoxicity

We have examined the cytotoxic effect of the cyclometallated iridium(III) polypyridine complexes towards HeLa cells using the MTT assay.[30] The IC_{50} values have been determined from the dose-dependence of surviving cells after exposure to the complexes for 48 h. The IC_{50} values of the iridium(III) complexes ranged from 4.0 to 9.8 μM (Table 7), which are significantly smaller than that of cisplatin (23.5 μM) under the same experimental conditions. In general, these complexes are similarly cytotoxic to related iridium(III) pq (Hpq = 2-phenylquinoline) complexes.[22a,b,d,f] It is interesting to note that there is a slight decrease in the IC_{50} values of complexes **3** and **4**, probably due to an increase of the lipophilicity

Table 7 IC_{50} values of the iridium(III) complexes

Complex	IC_{50}/μM
1	9.6 ± 0.5
2	9.8 ± 0.7
3	6.0 ± 0.9
4	4.0 ± 0.2
Cisplatin	23.5 ± 3.3

of the diimines. Although cytotoxicity is often a concern in cellular imaging studies, this drawback can be compensated by employing a low dose of the complex with a short incubation time with the cells. It is likely that further structural modification of this class of complexes such as the attachment of a poly(ethylene glycol) (PEG) pendant,[22g] can alleviate the cytotoxicity associated with the parent skeleton, while the desirable photophysical features of the complexes can be retained.

Cellular-uptake studies

HeLa cells loaded with the cyclometallated iridium(III) polypyridine complexes (5 μM) at 37 °C for 1 h have been analysed using laser-scanning confocal microscopy. The results for complex **4** are shown in Fig. 7. Upon excitation, the cells incubated with the complex displayed intense emission intensity, indicating efficient cellular internalisation of the complex molecules. The complex distribution in the cytoplasm was not even but localised in the perinuclear region, forming very sharp luminescent rings surrounding the nuclei. The nuclei showed much weaker emission, indicative of negligible nuclear uptake of the complex. From the image (Fig. 7), it is likely that the complex binds to hydrophobic organelles such as Golgi apparatus, endoplasmic reticulum and mitochondria.[31] Interestingly, incubation of the HeLa cells with complex **4** at 4 °C resulted in reduced cellular uptake efficiency as revealed by confocal microscopy (Fig. 8) and flow cytometry (Fig. 9). This suggests that an energy-requiring process should play a part in the cellular uptake process. The cellular uptake of complex **4** has been further investigated using different reagents including metabolic- and ATPase-inhibitors. The flow cytometric results are listed in Table 8. While most of the pretreatments did not result in any observable changes in the cellular uptake efficiency, incubation of HeLa cells with the metabolic inhibitor CCCP (20 μM) at 37 °C in a glucose-free medium before treatment with complex **4** led to a moderate decrease of cellular uptake efficiency (Table 8 and Fig. 9). Since CCCP inhibits oxidative phosphorylation, resulting in decreased ATP production and hence a lowered metabolic rate, the observed decrease of cellular uptake is in accordance with the argument that internalisation

Table 8 Flow cytometric results of HeLa cells incubated with complex **4** under various conditions for 1 h

Condition/inhibitor	Relative intensity (A. U.)
Blank	3.5
37 °C	100.0
4 °C	71.2
Nitrate (50 mM)	91.6
Vanadate (50 μM)	103.5
Molybdate (250 μM)	113.0
2-Deoxyglucose (50 mM)	115.5
Azide (3 mM)	109.6
CCCP (20 μM)	56.1

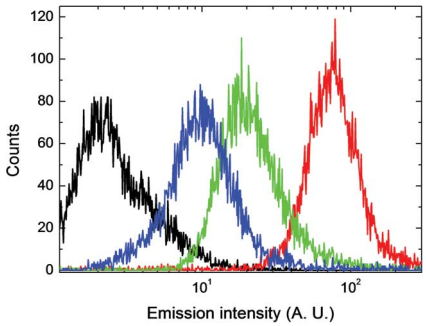

Fig. 9 Flow cytometric results of HeLa cells incubated with blank medium (black) and complex **4** for 1 h at 37 °C (red), 4 °C (green) and after pretreatment with CCCP at 37 °C (blue), respectively.

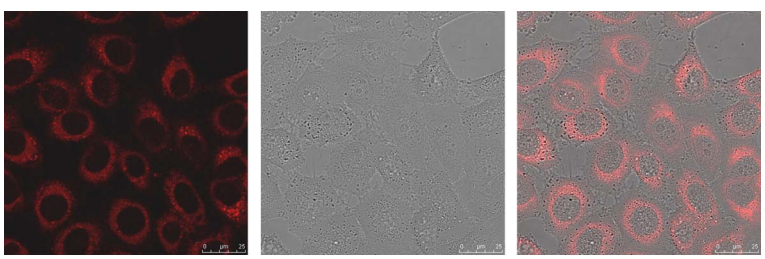

Fig. 7 Fluorescence (left), brightfield (middle), and overlaid (right) images of HeLa cells incubated with complex **4** (5 μM) at 37 °C for 1 h.

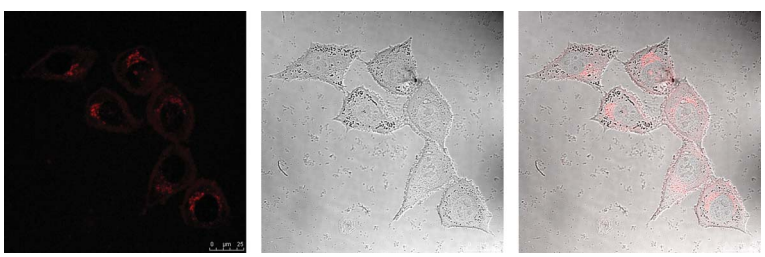

Fig. 8 Fluorescence (left), brightfield (middle), and overlaid (right) images of HeLa cells incubated with complex **4** (5 μM) at 4 °C for 1 h.

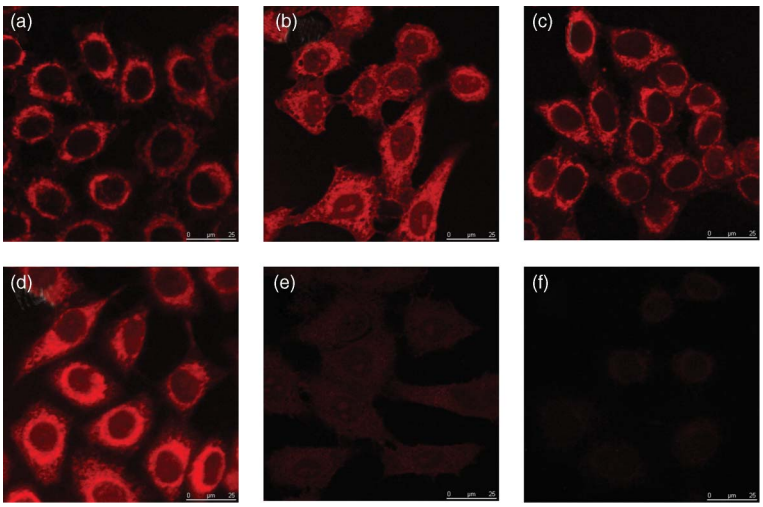

Fig. 10 Fluorescence images of HeLa cells incubated with complex **4** (5 μM) at 37 °C for 1 h (a) before and (b) after subsequent fixation with MeOH, or (c) fixation with paraformaldehyde, followed by extensive washing with MeOH; (d)–(f): fluorescence images of HeLa cells treated and fixed with the same procedures except that $[Ir(pq)_2(Ph_2\text{-phen})](PF_6)$ was used as the staining reagent.

of complex **4** occurred *via* an energy-requiring pathway such as endocytosis.[32]

The effects of the aldehyde groups of complex **4** on cellular labelling have been examined by fixed-cell imaging studies. HeLa cells were treated with complex **4** (at 37 °C for 1 h) and then fixed with MeOH. The confocal images showed that complex **4** was localised in the perinuclear region before (Fig. 10a) and after (Fig. 10b) the cells were fixed. Also, during the fixation, the complex diffused across the compromised nuclear envelop and stained the nuclear components including what appeared to be nucleoli. Remarkably, although many cellular reagents suffer from severe loss of staining ability after the cells are fixed with organic solvents, the emission intensity of the stained cells was retained after treatment with MeOH. This finding has been compared to the cell-staining properties of the aldehyde-free counterpart of complex **4**, $[Ir(pq)_2(Ph_2\text{-phen})](PF_6)$.[33] HeLa cells incubated with this pq complex at 37 °C for 1 h exhibited similar intracellular staining with an emission intensity that was similar to that of cells treated with complex **4** (Fig. 10d). This is in accordance with the results from ICP-MS analysis that revealed similar cellular uptake efficiencies for both complexes (the intracellular iridium contents of complex **4** and the pq complex were 0.38 and 0.39 fmol in an average cell, respectively). However, in sharp contrast to complex **4**, after the pq-complex-treated cells were fixed with MeOH, the emission intensity decreased significantly (Fig. 10e). The cellular staining properties of the two complexes have been further studied using paraformaldehye as the fixing reagent. HeLa cells were first stained by the complexes, then fixed by paraformaldehyde and extensively washed with MeOH. The confocal images showed that while the staining patterns of HeLa cells were similar to those under normal incubation of the two complexes, this fixation and washing treatment led to a significant decrease of emission intensity for the control complex (Fig. 10f). Remarkably, HeLa cells incubated with complex **4** with subsequent fixation and washing still displayed very intense emission intensity (Fig. 10c). Although the reasons for the drastic difference between the emission intensities of the fixed cells pretreated with the two complexes require more detailed investigations, since the only difference between the two complexes is the two aldehyde groups of complex **4**, it is conceivable that the amine-specific reactivity and protein cross-linking properties of the complex should play a key role in the cellular staining. It is possible that this complex, unlike its aldehyde-free counterpart, became anchored onto cellular structures (*e.g.*, *via* proteins on organelles) and was still retained even after the cells were extensively washed with MeOH. In summary, functionalisation of luminescent complexes with an aldehyde unit is useful for cellular staining experiments as it possibly allows covalent attachment of the imaging tools to the amine groups of various biomolecules as well as intracellular structures.

Conclusion

We report herein the synthesis, characterisation and photophysical and electrochemical properties of four luminescent cyclometallated iridium(III) bis(quinolylbenzaldehyde) diimine complexes. Flow cytometry and laser-scanning confocal microscopy studies revealed efficient uptake of complex **4** by HeLa cells and subsequent localisation in the perinuclear region. Results from temperature-dependence and inhibition experiments indicated that the internalisation mechanism was likely to be *via* endocytosis. The highly efficient internalisation of the complex at a low concentration in a relatively short incubation time and the fixed-cell confocal experiments suggests that these luminescent cyclometallated iridium(III) polypyridine complexes represent a new class of bio-imaging reagents.

Acknowledgements

We thank The Hong Kong Research Grants Council (Project No. CityU 102109) and City University of Hong Kong (Project No. 7002575) for financial support. The work described in this paper was also supported by a Special Equipment Grant from the Hong Kong University Grants Committee (SEG_CityU02).

P.-K. L. and M.-W. L acknowledge the receipt of a Postgraduate Studentship, a Research Tuition Scholarship and an Outstanding Academic Performance Award, all administered by City University of Hong Kong. We thank Mr. Kenneth King-Kwan Lau and Mr. Michael Wai-Lun Chiang for their assistance on the cellular experiments.

References

1 S. W. Botchway, M. Charnley, J. W. Haycock, A. W. Parker, D. L. Rochester, J. A. Weinstein and J. A. G. Williams, *Proc. Natl. Acad. Sci. U. S. A.*, 2008, **105**, 16071.

2 (*a*) P. M.-K. Siu, D.-L. Ma and C.-M. Che, *Chem. Commun.*, 2005, 1025; (*b*) D.-L. Ma, T. Y.-T. Shum, F. Zhang, C.-M. Che and M. Yang, *Chem. Commun.*, 2005, 4675; (*c*) P. Wu, E. L.-M. Wong, D. L. Ma, G. S.-M. Tong, K.-M. Ng and C.-M. Che, *Chem.–Eur. J.*, 2009, **15**, 3652.

3 (*a*) C. A. Puckett and J. K. Barton, *J. Am. Chem. Soc.*, 2007, **129**, 46; (*b*) C. A. Puckett and J. K. Barton, *Biochemistry*, 2008, **47**, 11711; (*c*) C. A. Puckett and J. K. Barton, *J. Am. Chem. Soc.*, 2009, **131**, 8738.

4 N. A. O'Connor, N. Stevens, D. Samaroo, M. R. Solomon, A. A. Marti, J. Dyer, H. Vishwasrao, D. L. Akins, E. R. Kandel and N. J. Turro, *Chem. Commun.*, 2009, 2640.

5 U. Neugebauer, Y. Pellegrin, M. Devocelle, R. J. Forster, W. Signac, N. Morand and T. E. Keyes, *Chem. Commun.*, 2008, 5307.

6 K. K.-W. Lo, T. K.-M. Lee, J. S.-Y. Lau, W.-L. Poon and S.-H. Cheng, *Inorg. Chem.*, 2008, **47**, 200.

7 (*a*) D.-L. Ma, C.-M. Che, F.-M. Siu, M. Yang and K.-Y. Wong, *Inorg. Chem.*, 2007, **46**, 740; (*b*) R. W.-Y. Sun, M. F.-Y. Ng, E. L.-M. Wong, J. Zhang, S. S.-Y. Chui, L. Shek, T.-C. Lau and C.-M. Che, *Dalton Trans.*, 2009, 10712.

8 K. A. Stephenson, S. R., T. Besanger, O. O. Sogbein, M. K. Levadala, N. McFarlane, J. A. Lemon, D. R. Boreham, K. P. Maresca, J. D. Brennan, J. W. Babich, J. Zubieta and J. Valliant, *J. Am. Chem. Soc.*, 2004, **126**, 8598.

9 (*a*) A. J. Amoroso, M. P. Coogan, J. E. Dunne, V. Fernández-Moreira, J. B. Hess, A. J. Hayes, D. Lloyd, C. Millet, S. J. A. Pope and C. Williams, *Chem. Commun.*, 2007, 3066; (*b*) A. J. Amoroso, R. J. Arthur, M. P. Coogan, J. B. Court, V. Fernández-Moreira, A. J. Hayes, D. Llyod, C. Millet and S. J. A. Pope, *New J. Chem.*, 2008, **32**, 1097.

10 (*a*) K. K.-W. Lo, M.-W. Louie, K.-S. Sze and J. S.-Y. Lau, *Inorg. Chem.*, 2008, **47**, 602; (*b*) M.-W. Louie, H.-W. Liu, M. H.-C. Lam, T.-C. Lau and K. K.-W. Lo, *Organometallics*, 2009, **28**, 4297; (*c*) M.-W. Louie, M. H.-C. Lam and K. K.-W. Lo, *Eur. J. Inorg. Chem.*, 2009, 4265.

11 J. Brunner and J. K. Barton, *Biochemistry*, 2006, **45**, 12295.

12 (*a*) C.-M. Che, R. W.-Y. Sun, W.-Y. Yu, C.-B. Ko, N. Zhu and H. Sun, *Chem. Commun.*, 2003, 1718; (*b*) C. K.-L. Li, R. W.-Y. Sun, S. C.-F. Kui, N. Zhu and C.-M. Che, *Chem.–Eur. J.*, 2006, **12**, 5253; (*c*) R. W.-Y. Sun, C. K.-L. Li, D.-L. Ma, J. J. Yan, C.-N. Lok, C.-H. Leung, N. Zhu and C.-M. Che, *Chem.–Eur. J.*, 2010, **16**, 3097.

13 K. A. King and R. J. Watts, *J. Am. Chem. Soc.*, 1987, **109**, 1589.

14 P. Didier, I. Ortmans, A. Kirsch-De Mesmaeker and R. J. Watts, *Inorg. Chem.*, 1993, **32**, 5239.

15 J.-P. Collin, I. M. Dixon, J.-P. Sauvage, J. A. G. Williams, F. Barigelletti and L. Flamigni, *J. Am. Chem. Soc.*, 1999, **121**, 5009.

16 (*a*) F. Neve, A. Crispini, S. Campagna and S. Serroni, *Inorg. Chem.*, 1999, **38**, 2250; (*b*) F. Neve, M. La Deda, A. Crispini, A. Bellusci, F. Puntoriero and S. Campagna, *Organometallics*, 2004, **23**, 5856.

17 (*a*) A. B. Tamayo, B. D. Alleyne, P. I. Djurovich, S. Lamansky, I. Tsyba, N. N. Ho, R. Bau and M. E. Thompson, *J. Am. Chem. Soc.*, 2003, **125**, 7377; (*b*) T. Sajoto, P. I. Djurovich, A. B. Tamayo, J. Oxgaard, W. A. Goodard III and M. E. Thompson, *J. Am. Chem. Soc.*, 2009, **131**, 9813; (*c*) A. F. Rausch, M. E. Thompson and H. Yersin, *Inorg. Chem.*, 2009, **48**, 1928.

18 I. Avilov, P. Minoofar, J. Cornil and L. De Cola, *J. Am. Chem. Soc.*, 2007, **129**, 8247.

19 (*a*) S.-J. Liu, Q. Zhao, R.-F. Chen, Y. Deng, Q.-L. Fan, F.-Y. Li, L.-H. Wang and C.-H. Huang, *Chem.–Eur. J.*, 2006, **12**, 4351; (*b*) X. Li, Z. Chen, Q. Zhao, L. Shen, F. Li, T. Yi, Y. Cao and C. Huang, *Inorg. Chem.*, 2007, **46**, 5518.

20 (*a*) K. K.-W. Lo, C.-K. Chung and N. Zhu, *Chem.–Eur. J.*, 2003, **9**, 475; (*b*) K. K.-W. Lo, C.-K. Chung, T. K.-M. Lee, L.-H Lui, K. H.-K. Tsang and N. Zhu, *Inorg. Chem.*, 2003, **42**, 6886; (*c*) K. K.-W. Lo, C.-K. Li and J. S.-Y. Lau, *Organometallics*, 2005, **24**, 4594; (*d*) K. K.-W. Lo, C.-K. Chung and N. Zhu, *Chem.–Eur. J.*, 2006, **12**, 1500; (*e*) K. K.-W. Lo, K. Y. Zhang, C.-K. Chung and K. Y. Kwok, *Chem.–Eur. J.*, 2007, **13**, 7110; (*f*) K. K.-W. Lo, K. Y. Zhang, S.-K. Leung and M.-C. Tang, *Angew. Chem., Int. Ed.*, 2008, **47**, 2213.

21 (*a*) M. Yu, Q. Zhao, L. Shi, F. Li, Z. Zhou, H. Yang, T. Yi and C. Huang, *Chem. Commun.*, 2008, 2115.

22 (*a*) K. K.-W Lo, P.-K. Lee and J. S.-Y. Lau, *Organometallics*, 2008, **27**, 2998; (*b*) J. S.-Y. Lau, P.-K. Lee, K. H.-K. Tsang, C. H.-C. Ng, Y.-W. Lam, S.-H. Cheng and K. K.-W. Lo, *Inorg. Chem.*, 2009, **48**, 708; (*c*) K. Y. Zhang and K. K.-W. Lo, *Inorg. Chem.*, 2009, **48**, 6011; (*d*) K. Y. Zhang, S. P.-Y. Li, N. Zhu, I. W.-S. Or, M. S.-H. Cheung, Y.-W. Lam and K. K.-W. Lo, *Inorg. Chem.*, 2010, **49**, 2530; (*e*) S.-K. Leung, K. Y. Kwong, K. Y. Zhang and K. K.-W. Lo, *Inorg. Chem.*, 2010, **49**, 4984; (*f*) K. Y. Zhang, H.-W. Liu, T. T.-H. Fong, X.-G. Chen and K. K.-W. Lo, *Inorg. Chem.*, 2010, **49**, 5432; (*g*) S. P.-Y. Li, H.-W. Liu, K. Y. Zhang and K. K.-W. Lo, *Chem.–Eur. J.*, 2010, **16**, 8329.

23 D. D. Perrin and W. L. F. Armarego, *Purification of Laboratory Chemicals*, 3rd Ed.; Pergamon Press, New York, 1988.

24 T. Kolasa, D. E. Gunn, P. Bhatia, K. W. Woods, T. Gane, A. O. Stewart, J. B. Bouska, R. R. Harris, K. I. Hulkower, P. E. Malo, R. L. Bell, G. W. Carter and C. D. W. Brooks, *J. Med. Chem.*, 2000, **43**, 690.

25 J. N. Demas and G. A. Crosby, *J. Phys. Chem.*, 1971, **75**, 991.

26 K. Nakamaru, *Bull. Chem. Soc. Jpn.*, 1982, **55**, 2697.

27 *CrysAlis*, Oxford Diffraction Ltd., Version 1.171.33.46, 2990.

28 G. M. Sheldrick, *SHELXS97 and SHELXL97*, Program for Crystal Structure Solution and Refinements, University of Göttingen, Germany, 1997.

29 L. J. Farrugia, *J. Appl. Crystallogr.*, 1999, **32**, 837.

30 T. Mosmann, *J. Immunol. Methods*, 1983, **65**, 55.

31 (*a*) T. Kobayashi and Y. Arakawa, *J. Cell Biol.*, 1991, **113**, 235; (*b*) R. E. Pagano, O. C. Martin, H.-C. Kang and R. P. Haugland, *J. Cell Biol.*, 1991, **113**, 1267.

32 (*a*) E. Reaven, L. Tsai and S. Azhar, *J. Biol. Chem.*, 1996, **271**, 16208; (*b*) D. J. Weaver, Jr. and E. W. Voss, *Biol. Cell*, 1998, **90**, 169; (*c*) A. Dautry-Varsat, A. Ciechanover and H. F. Lodish, *Proc. Natl. Acad. Sci. U. S. A.*, 1983, **80**, 2258.

33 C. Dragonetti, L. Falciola, P. Mussini, S. Righetto, D. Roberto, R. Ugo, A. Valore, F. De Angelis, S. Fantacci, A. Sgamellotti, M. Ramon and M. Muccini, *Inorg. Chem.*, 2007, **46**, 8533.